Soft Matter

RSC Publishing

PAPER

High-order jamming crossovers and density anomalies

Cite this: *Soft Matter*, 2013, **9**, 9557

Massimo Pica Ciamarra*[a] and Peter Sollich[b]

Received 29th May 2013
Accepted 5th August 2013

DOI: 10.1039/c3sm51505b

www.rsc.org/softmatter

We demonstrate that particles interacting *via* core-softened potentials exhibit a series of successive density anomalies upon isothermal compression, leading to oscillations in the diffusivity and thermal expansion coefficient, with the latter reaching negative values. These finite-temperature density anomalies are then shown to correspond to zero-temperature high-order jamming crossovers. These occur when particles are forced to come into contact with neighbours in successive coordination shells upon increasing the density. The crossovers induce anomalous behavior of the bulk modulus, which oscillates with density. We rationalize the dependence of these crossovers on the softness of the interaction potential, and relate the jamming crossovers and the anomalous diffusivity *via* the properties of the vibrational spectrum.

1 Introduction

Core-softened interaction potentials, such as the Hertzian and the Gaussian interaction, have been used to model athermal systems like emulsions, bubble rafts[1] and granular materials,[2] as well as ultrasoft colloidal particles[3] where thermal effects are essential, such as star-polymers[4–6] and microgels.[7–10] As a result, the properties of particle systems with core-softened interactions have been studied both at zero and at finite temperature.

At zero temperature, particles interacting *via* core-softened potentials of a finite range exhibit a jamming transition when the volume fraction crosses a threshold ϕ_J; see ref. 2 and 11 for recent reviews. At the jamming transition the system acquires mechanical rigidity due to the emergence of a percolating network of contacts. The average number of contacts per particle, Z, quantifies the connectivity of this network. It is zero for $\phi < \phi_J$ and jumps at ϕ_J to the isostatic value Z_{iso}, which is the minimum value consistent with the requirement of mechanical stability. Physically, above the jamming transition each particle is forced to touch particles in its first coordination shell. The excess contact number $\Delta Z = Z - Z_{iso}$ grows as a power law in $\phi - \phi_J$, and is related to a length scale, the isostatic length, diverging at the transition as ΔZ^{-1}. This length scale is associated with the non-affine response of the system,[12] and is related to an abundance of soft vibrational modes observed close to jamming. Indeed, the density of states $D(\omega)$ satisfies Debye scaling up to a characteristic frequency scaling as $\omega^* \propto \Delta Z$, above which it flattens.

At finite temperature, core-softened potentials give rise to a density anomaly.[13–16] A density anomaly is a region of the phase diagram where the diffusivity increases upon isothermal compression, which usually overlaps with a region characterized by a negative thermal expansion coefficient. Density anomalies are also observed when a core-softened potential is modified *via* the addition of a small hard-core radius. Indeed, potentials with these features, like the Jagla potential,[17] are the simplest models of atomic liquids with density anomalies, such as water; see ref. 18 for a recent review. In network-forming liquids, these anomalies are related to soft vibrational modes characterized by a rigid rotation of tetrahedral structures, known as rigid unit modes.[19]

Even though an abundance of soft modes characterizes both the jamming transition and the density anomalies, these two phenomena have not been related before, possibly because density anomalies occur at volume fractions well above ϕ_J.[13–17,20] Here we show that there exists a profound relationship between these two phenomena. We show that the jamming transition is the first of a series of high-order jamming crossovers that occur on increasing the volume fraction as particles come into contact with those of subsequent coordination shells. The geometric signatures of the jamming crossovers are oscillations in the rate of formation of new contacts on compression. The mechanical ones include an anomalous volume fraction dependence of the elasticity of the system, whereby the bulk and shear moduli depend on the volume fraction in an oscillatory fashion. This implies, surprisingly, that away from the jamming transition there is no simple relationship between the mechanical moduli and the connectivity. We show that density anomalies are the finite temperature counterpart of the jamming crossovers, and clarify the relationship between these phenomena by studying the soft vibrational modes. Our results lead to a simple geometric explanation for density anomalies like those in soft particle systems such as many-armed star polymers,[21] with possible implications also for anomalies in network-forming liquids[18] such as water.

[a]CNR–SPIN, Dipartimento di Scienze Fisiche, University of Napoli Federico II, Italy. E-mail: massimo.picaciamarra@na.infn.it

[b]King's College London, Department of Mathematics, Strand, London WC2R 2LS, UK

2 Model

We perform molecular dynamics simulations of 50 : 50 binary mixtures of particles with diameter $D_l = 1$ and $D_s = D_l/1.4$ and mass $M = 1$, in two dimensions. Two particles i and j interact if they have a positive overlap, $\delta_{ij} = D_{ij} - r_{ij} > 0$, where D_{ij} is their average diameter and r_{ij} is the distance between them. When this is the case the interaction potential is

$$V(\delta_{ij}) = \frac{1}{\alpha} k \left(\frac{\delta_{ij}}{D_l}\right)^{\alpha}. \quad (1)$$

The parameter α controls the softness of the interaction potential, with larger values of α corresponding to softer potentials. M, D_l and $k = 1$ are our units of mass, length and energy. Finite temperature simulations have been performed in the NVT and NPT ensembles, for systems of $N = 10^3$ particles. Zero temperature properties have been investigated by quenching random configurations of $N = 10^4$ particles to the closest energy minimum *via* the conjugate-gradient algorithm.[22] We analyse a large volume fraction range, varying the volume fraction from the jamming threshold at $\phi \simeq 0.84$ up to $\phi = 3$, and consider $\alpha = 1.25$,1.5,1.75,2 (Harmonic), 2.5 (Hertzian), 3 and 10.

For $\alpha = 1$ our model reduces to the cut-ramp potential,[23] a variant of the Jagla potential.[17] The latter has been used extensively in the study of water-like density anomalies.[18] More generally for $\alpha < 2$, eqn (1) implies a divergence of the bond stiffness $k(\delta) = V''(\delta)$ for $\delta \to 0^+$. Regularization of this divergence[24] does not qualitatively affect our results, and leads to a bond stiffness that has a maximum as a function of δ. Potentials with such behaviour, e.g. the Gaussian potential, have been used to model some polymeric particles[3] and anomalous liquids.[18]

3 Result

3.1 $T > 0$ properties

We start by showing that systems of particles interacting *via* purely repulsive finite range potentials are not characterized by a single density anomaly as previously reported,[13–17,20] but by a series of such anomalies. Indeed, as illustrated in Fig. 1a, there exist successive volume fraction ranges in which the diffusivity increases upon isothermal compression. An analogous result has been observed in models of polymer stars.[21] Likewise, Fig. 1b shows the existence of multiple volume fraction ranges characterized by a negative volumetric thermal expansion coefficient. We have computed this thermal expansion coefficient $\frac{1}{V}\frac{dV}{dT}$ by monitoring the temperature dependence of the volume in the NPT ensemble. To better highlight the relationship with the jamming crossovers, we show in Fig. 1b its dependence on the volume fraction, rather than the pressure. This is obtained by computing, for each value of ϕ, the thermal expansion coefficient at the value of the pressure at which the average volume fraction is ϕ. The diffusivity anomalies and those of the thermal expansion coefficient depend on the interaction potential, and their number and strength decrease on increasing α. Indeed, no anomalies are observed for $\alpha = 10$. Likewise, the anomalies disappear at higher temperatures. In the following, we clarify the microscopic origin of these anomalies and show that they are the finite temperature counterparts of high-order jamming crossovers.

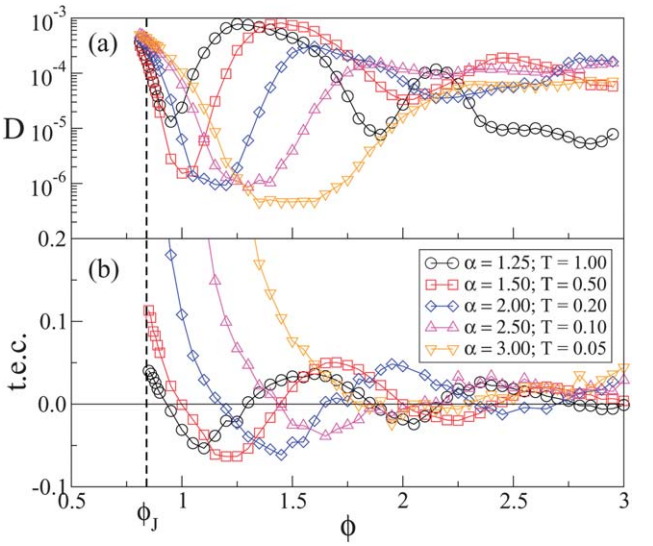

Fig. 1 (a) Volume fraction dependence of the diffusion coefficient averaged over the two species, for different interaction potentials. For each potential, the temperature is chosen so that the minimum value of D in the range of ϕ studied here is $D \simeq 10^{-6}$. (b) Thermal expansion coefficient.

3.2 $T = 0$ properties

We have determined the geometric and mechanical properties of jammed configurations in a large volume fraction range, considering ϕ values with a spacing of $\Delta\phi = 5 \times 10^{-2}$ far from the jamming transition and $\Delta\phi = 10^{-2}$ close to it; data are averaged over 50 independent jammed configurations for each value of ϕ. Piecewise polynomial interpolations of the average contact number Z and of the pressure P have been used to estimate $dZ/d\phi$ and the bulk modulus $K = \phi dP/d\phi$. The same prescription would give K in isothermal simulations at $T > 0$, which motivates its use also for our jammed configurations. Further support comes from the fact that the pressure as a function of volume fraction for the latter agrees closely with the low-T extrapolation of isothermal data (not shown).

Fig. 2a illustrates the volume fraction dependence of the mean contact number and its first derivative. At the jamming transition, these quantities behave as expected, increasing in a singular fashion as the first nearest-neighbor particle contacts are formed.[2] At higher volume fractions $dZ/d\phi$ varies in an oscillatory manner. Its successive peaks can be interpreted as high-order jamming crossovers, during which particles establish contacts with neighbors in successive coordination shells. If one assumes that beyond the jamming transition the system deforms affinely, then the oscillations in $dZ/d\phi$ are seen to correspond to peaks in the radial distribution function of the initial distribution; these weaken at larger distances and correspondingly $dZ/d\phi$ flattens out at large ϕ so that Z increases linearly with ϕ. As an aside we

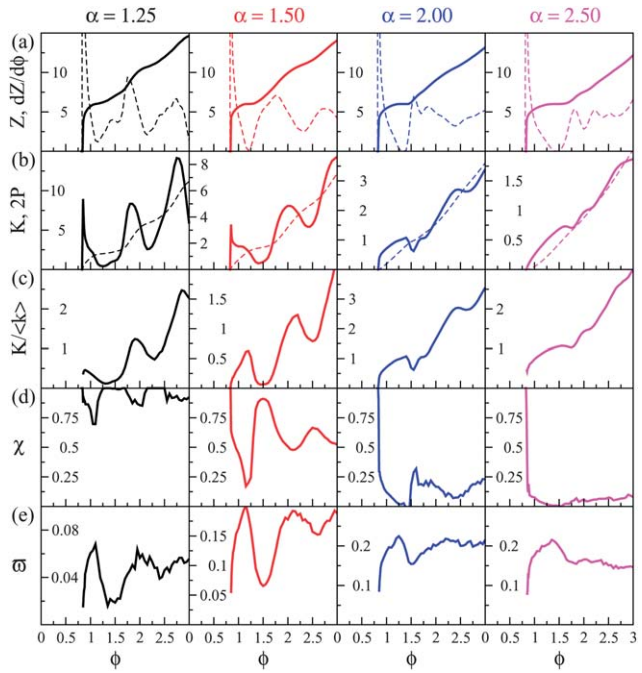

Fig. 2 Volume fraction dependence of (a) mean contact number Z (full line) and its volume fraction derivative $dZ/d\phi$ (dashed line), (b) pressure P (dashed line) and the bulk modulus K (full line), (c) normalized bulk modulus $K/\langle k\rangle$, (d) non-affinity parameter χ, and (e) normalized characteristic frequency ϖ. Each column refers to a different value of α, as indicated.

note that for soft potentials there is a volume fraction range where the average contact number is constant, $Z = 6$; here all particles in contact are Vöronoi neighbors, and the value $Z = 6$ is fixed by Euler's theorem for planar graphs.[25]

The jamming crossovers also influence mechanical properties such as the pressure P and the bulk modulus K, whose volume fraction dependence is shown in Fig. 2b. The pressure increases most strongly where $dZ/d\phi$ is large, *i.e.* where most new contacts are being created. The behaviour of K is more surprising, and demonstrates that an interpretation in terms of affine deformation on compression is too simplistic: rather than simply increasing as new bonds are formed, K exhibits a series of peaks and troughs upon increasing the density. Note that for $\alpha < 2$, where bonds are stiffest when initially formed, K is expected to decrease above the jamming transition before increasing again. One can remove this effect by normalizing the bulk modulus with the average bond stiffness, $\langle k\rangle \propto \langle\delta^{\alpha-2}\rangle$; as Fig. 2c shows, this normalized K no longer diverges near jamming but the oscillatory variation at higher density that is of interest here persists. The oscillations in K must therefore be attributed to structural changes induced by the crossovers. We note, however, that the results of Fig. 2 do not support the conjecture of a phase transition at a volume fraction $\phi_d > \phi_J$.[26]

We elucidate the structural changes occurring at the jamming crossovers by investigating the volume fraction dependence of the overlap p.d.f. $P_Z(\delta)$, normalized across the interacting particles so that $\int_0^1 P_Z(\delta)d\delta = Z$. This quantity characterizes the geometrical structure of the system by focusing on the overlaps. These are of course directly related to the interparticle distances. For a monodisperse system this gives a simple relation to the radial distribution function, namely $P_Z(\delta) \propto (D-\delta)^{d-1}g(D-\delta)$ in spatial dimension d. In our mixture a similar relation holds, but the correspondence between distance r and overlap δ depends on the size of the interacting particles. The advantage of $P_Z(\delta)$ is that it tells us directly how far each particle pair is from contact ($\delta = 0$), independent of the particle sizes.

Since $dZ/d\phi$ increases when particles start interacting with those of a new shell, we show in Fig. 3 $P_Z(\delta)$ at volume fractions immediately following that of the first minimum of $dZ/d\phi$, for different values of α. For $\alpha = 3$ the formation of new contacts does not have a strong effect on the distribution. $P_Z(\delta)$ is simply shifted towards larger values of δ, which suggests a mostly affine deformation. For $\alpha = 2$, on the other hand, the formation of new contacts leads to a transformation of $P_Z(\delta)$, the net outcome of which is the creation of a new peak at small positive δ. This peak shifts towards positive δ values on further compressing the system. At smaller α, $P_Z(\delta)$ has a diverging peak at $\delta \to 0^+$, and the transformation of the distribution driven by contact formation leads to an increase of this peak. The jamming crossovers of higher order lead to analogous changes in $P_Z(\delta)$. These results clarify that the jamming crossovers lead to a rearrangement of the geometric structure of the system, which is more pronounced for smaller α. Experimentally, signatures of this behaviour should be visible in the evolution of the structure factor on compression. In particular, we note that on increasing the volume fraction, the shell structure that we observe in $P_Z(\delta)$ for $\delta < 0$ is transformed into a shell structure for *positive* overlaps for large α, while conversely it is washed out for smaller α.

To explain the role of the softness of the interaction potential in determining the shape of the overlap probability distribution, we introduce the concept of intersection volume fraction $\phi_\cap$. We define $\phi_\cap$ as the sum of the volumes of intersection of

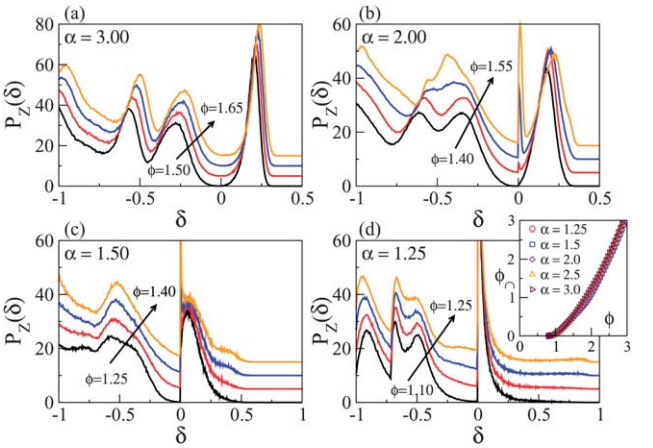

Fig. 3 Panels (a–c): overlap probability distribution function $P_Z(\delta)$ for different values of the volume fraction separated by $\Delta\phi = 5 \times 10^{-2}$, as indicated. Data are shifted vertically for clarity. A negative δ corresponds to the distance between the surfaces of non-interacting particles. The inset of panel (d) shows that the intersection volume fraction $\phi_\cap$ is to a good approximation independent of the softness of the interaction α, specified in the legend.

any pair of interacting particles, normalized by the total volume of the system. Close to the jamming transition, where the intersection volumes do not themselves overlap, $\phi = \phi_J + \phi_\cap$, so $\phi_\cap$ is linearly dependent on ϕ and potentially independent. In addition, here $\phi_\cap(\phi)$ scales as the q-th moment of $P_Z(\delta)$, $\phi_\cap \propto \langle\delta^q\rangle$, as the volume of intersection of two particles grows as δ^q for small δ, where $q = 1.5$. Fig. 3d (inset) shows that $\phi_\cap$ is approximately potential-independent also at higher volume fractions, so we can regard it as being fixed by ϕ throughout. The energy of the system, on the other hand, scales as the α-th moment of $P_Z(\delta)$, $E \propto \langle\delta^\alpha\rangle$. Accordingly, constant-$\phi$ energy minimization protocols search for a P_Z distribution that minimizes $\langle\delta^\alpha\rangle$ subject to the constraint of constant $\langle\delta^q\rangle$, or more generally of constant intersection volume fraction away from jamming. The effect of α on the outcome can be understood by considering the energy $e(\delta_i, \delta_j) = (\delta_i^\alpha + \delta_j^\alpha)/\alpha$ of two overlaps δ_i and δ_j related to the constraint of constant intersection volume fraction, $\delta_i^q + \delta_j^q = \text{const}$. Then for $\alpha > q$ it is energetically more favourable for the system to make the overlaps equal, while for $\alpha > q$ the energy is minimized by making them maximally different. This finding explains the abundance of small contacts in the overlap distribution for small α, and the qualitative change in P_Z as α crosses q.

The overlap distribution indicates that the smaller the value of α, the more heterogeneous the structure of the system is. This suggests an increase of the non-affine response of the system on decreasing α. We estimate the degree of affinity of the system by comparing the actual bulk modulus K with that computed in the affine (Born) approximation, K_{aff}. If the system responds affinely to the compression, then $K = K_{\text{aff}}$, otherwise $K < K_{\text{aff}}$. Accordingly, the strength of the non-affine response, *i.e.* the relevance of the fluctuation term of the stress tensor,[27] can be quantified *via* the parameter

$$\chi = \frac{K_{\text{aff}} - K}{K_{\text{aff}}}, \quad 0 \le \chi \le 1.$$

Then $\chi = 0$ when the response is affine, while $\chi \to 1$ when the response is highly non-affine. Fig. 2d confirms the expectation that stiffer potentials (small α) give rise to a less affine response: the typical value of χ decreases on increasing α. In addition, the comparison of Fig. 2c and d reveals the presence of a clear anticorrelation between χ and K, which indicates that the jamming crossovers induce an increase of the degree of non-affinity of the system, much like the jamming transition. We also note that the oscillations of $\chi(\phi)$ suggest that the non-affine correlation length that diverges at the jamming transition[2,11] is a non-monotonic function of the volume fraction.

We close this section with some remarks on how the modulus K should be determined. Above, we have defined it from the change in pressure between the two ensembles of jammed configurations at two neighbouring values of the volume fraction. Alternatively, one could measure K by compressing individual configurations and monitoring the change in pressure. This procedure gives very similar results to those shown above, provided one uses volume fraction changes $\Delta\phi$ obeying $1/N \ll \Delta\phi \ll 1$. These conditions ensure that one gets a result that is well-defined in the thermodynamic limit: the volume fraction change must be small but the absolute change in volume large. Such $\Delta\phi$ lead to compression avalanches, as discussed in more detail in ref. 28. Taking infinitesimal $\Delta\phi$, on the other hand, would exclude this effect and so over-estimate the modulus. This is the method that was used to measure the modulus in ref. 26, and may be the reason why anomalies in the modulus were not observed in that work; another reason could be a slight difference in the inter-particle potential, which in ref. 26 is scaled by $\sigma_{ij}^{-\alpha}$, giving smaller repulsion for the larger particles.

3.3 Connecting $T = 0$ and $T > 0$

The mechanical anomalies observed at $T = 0$, and the dynamical ones observed at $T > 0$, exhibit closely related volume fraction dependences. This suggests that they have the same physical origin. We elucidate this mechanism by exploiting recent results correlating the thermal[29] and shear[30,31] induced relaxation of glassy systems, and their vibrational modes. These studies have shown that relaxation proceeds through localized events, which occur where the low frequency modes are quasi-localized. In this picture, low-frequency modes are defects allowing for the relaxation of disordered particle systems.[31] In particular, since the activation energy of a soft mode is correlated with its eigenfrequency,[32] one expects the dynamics to speed up when the typical frequency of the soft modes decreases. To check this expectation we have determined the eigenfrequencies by numerically diagonalizing the Hessian, and then studied the volume fraction dependence of the average eigenfrequency ϖ of the lowest 5% of modes, normalized by the average eigenfrequency of all modes. Results are illustrated in Fig. 2e, for different interaction potentials. ϖ exhibits oscillations as the volume fraction increases, which are anti-correlated with those of the diffusion coefficient. In addition, ϖ is strongly anti-correlated with the parameter χ. These results confirm the important role of the soft modes in determining both the relaxation dynamics and the mechanical properties of the system. The emergence of soft modes on increasing the volume fraction is surprising. In analogy with what is observed in network-forming liquids, where density anomalies are related to the presence of soft vibrational modes characterized by a rigid rotation of stiff tetrahedral structures,[19] one might speculate that the soft modes emerging in our system on compression are also characterized by coordinated rigid rotation of particle clusters.

4 Conclusions

We have demonstrated the existence of high-order jamming crossovers in soft particle systems with increasing density. These occur when particles start to come into contact with neighbors in subsequent coordination shells. This increased connectivity can lead, surprisingly, to softening of the system, because of strongly non-affine deformation. The mechanical manifestation of these crossovers is the anomalous behavior of elastic properties such as the bulk and shear (data not shown) moduli, which vary in an oscillatory manner with the volume fraction. The crossovers also manifest themselves dynamically,

as density anomalies like those observed in water and in other network forming liquids. These anomalies include both an increased diffusivity on compression and a negative thermal expansion coefficient. Our results provide a simple geometric interpretation of these anomalies. We have related the $T = 0$ and the $T > 0$ anomalies to the emergence of soft vibrational modes around the crossovers, confirming their important role in the relaxation dynamics.[29–31] These results suggest that the scaling relation between relaxation time and vibrational dynamics found in normal liquids[33] may also hold for anomalous liquids. We note that the anomalies are observed at the high-order jamming crossovers, and not at the jamming transition, where the diffusion coefficient decreases monotonically on compression. One may speculate that this is so because at the jamming crossovers there is a coexistence of compressed bonds, and of new almost uncompressed bonds. These bonds may play the role of the two interaction length scales which are known to induce dynamical anomalies in models of water,[18] and are responsible for the rigid unit modes leading to a negative thermal expansion coefficient in network forming systems.[19] These two length scales are not present at the jamming transition. In this respect, it would be interesting to investigate the spatial structure of the soft modes at the jamming crossovers. Finally, we note that we have obtained analogous results to those shown in this paper also for other mixtures, *e.g.* polydisperse systems where particle sizes are drawn from a continuous distribution,[25] and in three rather than two dimensions. In the latter case we used monodisperse, *i.e.* uniformly sized, particles but still observe anomalies that are qualitatively similar to those in the two-dimensional mixtures. This rules out one hypothetical explanation for these anomalies, namely that it is the different particle sizes that create a competition between different length scales.

Acknowledgements

MPC thanks the Dept. of Mathematics, King's College London for hospitality, and MIUR-FIRB RBFR081IUK for financial support.

References

1 D. J. Durian, *Phys. Rev. Lett.*, 1995, **75**, 4780.
2 M. van Hecke, *J. Phys.: Condens. Matter*, 2010, **22**, 033101.
3 A. Jusufi, J. Dzubiella, C. N. Likos, C. von Ferber and H. Lowen, *J. Phys.: Condens. Matter*, 2001, **13**, 6177; C. N. Likos, *Soft Matter*, 2006, **2**, 478.
4 C. N. Likos, H. Löwen, M. Watzlawek, B. Abbas, O. Jucknischke, J. Allgaier and D. Richter, *Phys. Rev. Lett.*, 1998, **80**, 4450.
5 E. Zaccarelli, C. Mayer, A. Asteriadi, C. N. Likos, F. Sciortino, J. Roovers, H. Iatrou, N. Hadjichristidis, P. Tartaglia, H. Löwen and D. Vlassopoulos, *Phys. Rev. Lett.*, 2005, **95**, 268301.
6 E. Stiakakis, A. Wilk, J. Kohlbrecher, D. Vlassopoulos and G. Petekidis, *Phys. Rev. E: Stat., Nonlinear, Soft Matter Phys.*, 2010, **81**, 020402.
7 B. R. Saunders and B. Vincent, *Adv. Colloid Interface Sci.*, 1999, **80**, 1.
8 H. Senff and W. Richtering, *J. Chem. Phys.*, 1999, **111**, 1705.
9 J.-J. Lietor-Santos, B. Sierra-Martin, R. Vavrin, Z. Hu, U. Gasser and A. Fernandez-Nieves, *Macromolecules*, 2009, **42**, 6225.
10 D. Coslovich and A. Ikeda, *Soft Matter*, 2013, **9**, 6786.
11 A. J. Liu and S. R. Nagel, *Annu. Rev. Condens. Matter Phys.*, 2010, **1**, 14.
12 W. G. Ellenbroek, Z. Zeravcic, W. van Saarloos and M. van Hecke, *Europhys. Lett.*, 2009, **87**, 34004.
13 P. Mausbach and H. O. May, *Fluid Phase Equilib.*, 2006, **249**, 17.
14 L. Berthier, A. J. Moreno and G. Szamel, *Phys. Rev. E: Stat., Nonlinear, Soft Matter Phys.*, 2010, **82**, 060501(R).
15 L. Wang, Y. Duan and N. Xu, *Soft Matter*, 2012, **8**, 11831.
16 F. H. Stillinger and D. K. Stillinger, *Phys. A*, 1997, **244**, 358.
17 E. A. Jagla, *J. Chem. Phys.*, 1999, **111**, 8980; *J. Phys. Chem.*, 1999, **11**, 10251; *Phys. Rev. E: Stat., Nonlinear, Soft Matter Phys.*, 2001, **63**, 061509.
18 S. V. Buldyrev, G. Malescio, C. A. Angell, N. Giovambattista, S. Prestipino, F. Saija, H. E. Stanley and L. Xu, *J. Phys.: Condens. Matter*, 2009, **21**, 504106; G. Malescio, *J. Phys.: Condens. Matter*, 2007, **19**, 073101.
19 M. T. Dove, *Phase Transitions*, 1997, **61**, 1.
20 Z. Yan, S. V. Buldyrev, N. Giovambattista and H. E. Stanley, *Phys. Rev. Lett.*, 2005, **95**, 130604.
21 G. Foffi, *et al.*, *Phys. Rev. Lett.*, 2003, **90**, 238301.
22 C. S. O'Hern, *et al.*, *Phys. Rev. Lett.*, 2002, **88**, 075507.
23 E. Lascaris, G. Malescio, S. V. Buldyrev and H. E. Stanley, *Phys. Rev. E: Stat., Nonlinear, Soft Matter Phys.*, 2010, **81**, 031201.
24 We checked this by considering the potential $W(\delta,\alpha) = V(\delta,2)\exp(-\delta/\delta_0) + V(\delta,\alpha)(1 - \exp(-\delta/\delta_0))$, with $\delta_0/D_1 = 510^{-2}$, which regularizes the bulk modulus for $\alpha < 2$.
25 M. P. Ciamarra and P. Sollich, *J. Chem. Phys.*, 2013, **138**, 12A529.
26 C. Zhao, K. Tian and N. Xu, *Phys. Rev. Lett.*, 2011, **106**, 125503.
27 D. R. Squire, A. C. Holt and W. G. Hoover, *Physica A*, 1969, **42**, 388; J.-L. Barrat, J.-N. Roux, J.-P. Hansen and M. L. Klein, *Europhys. Lett.*, 1988, **7**, 707.
28 M. Pica Ciamarra and P. Sollich, *AIP Conf. Proc.*, 2013, **176**, 1518.
29 A. Widmer-Cooper and P. Harrowell, *J. Phys.: Condens. Matter*, 2005, **17**, S4025; A. Widmer-Cooper, *et al.*, *Nat. Phys.*, 2008, **4**, 711.
30 M. Tsamados, A. Tanguy, F. Lèonforte and J. L. Barrat, *Eur. Phys. J. E*, 2008, **26**, 283; A. Tanguy, B. Mantisi, and M. Tsamados, *Europhys. Lett.*, **2010**, 90, 16004.
31 M. L. Manning and A. J. Liu, *Phys. Rev. Lett.*, 2011, **107**, 108302.
32 N. Xu, V. Vitelli, A. J. Liu and S. R. Nagel, *Europhys. Lett.*, 2010, **90**, 56001.
33 L. Larini, A. Ottochian, C. De Michele and D. Leporini, *Nat. Phys.*, 2008, **4**, 42.